Design and Modeling of Application Specific Optical Waveguides

A Dissertation submitted towards the partial fulfilment of the requirement for the award of degree of

Master of Technology in
Nanoscience and Technology

Submitted by

Himanshu Pandey
2K14/NST/03

Under the supervision of

Dr. Ajeet Kumar
Assistant Professor

Department of Applied Physics
Delhi Technological University
(Formerly Delhi College of Engineering)

JUNE 2016

DELHI TECHNOLOGICAL UNIVERSITY

Established by Govt. Of Delhi vide Act 6 of 2009
(Formerly Delhi College of Engineering)
Shahbad Daulatpur, Bawana, Delhi-110042

CERTIFICATE

This is to certify that work which is being presented in the dissertation entitled **"Design and Modeling of Application Specific Optical Waveguides"** is authentic work of **Himanshu Pandey** under my guidance and supervision in the partial fulfilment of requirement towards the degree of **Master of Technology in Nanoscience and Technology** run by Department of Applied Physics in Delhi Technological University during the year 2014-2016.

As per the candidate declaration this work has not been submitted elsewhere for the award of any other degree.

Dr. Ajeet Kumar
Supervisor, Assistant Professor
Department of Applied Physics

Dr. S.C Sharma
Professor and Head of Department
Department of Applied Physics

DECLARATION

I hereby declare that all the information in this document has been obtained and presented in accordance with the academic rules and ethical conduct. This report is my own, unaided work. I have fully cited and referenced all material and results that are not original to this work. It is being submitted for the degree of Master of Technology in Nanoscience and Technology at Delhi Technological University. It has not been submitted for any degree or examination in any other university.

Himanshu Pandey
M. Tech. NST
2K14/NST/03

ABSTRACT

Integrated-optic waveguide lasers have been a matter of considerable attention for research because of their unique features, such as compactness and possibility of integrating single mode waveguide are usually employed in such lasers to avoid mode competition and intermodal dispersion. Hence, in this report a multi-trench leaky channel waveguide design is presented that supports an effective single guided mode. The waveguide works on the principle of higher-order mode discrimination. The structure is analysed by the finite-element method and the leakage loss of the modes along with the effective mode area have been calculated. It is shown that waveguide formed in silica with core width of 4 μm can exhibit single mode operation at 1550 nm wavelength. Numerical results show that wavelength ensure extended single mode operation in the wavelength range of 1.25-2.0 μm with a rectangular core area as large as 50 μm^2.

A theoretical investigation of a promising design of highly nonlinear As_2Se_3 based Chalcogenide waveguide is reported for generation of tunable slow light and its application at 1550 nm. The effective mode area and the confinement loss have been observed by varying the half width and height of the core of waveguide. Hence, the maximum allowable pump power for undistorted output pulse and time-delay experienced by the pulse propagating in designed waveguide are simulated. It has been observed that, in a 10 cm long Chalcogenide (As_2Se_3), the time-delay of ~252 ns can be obtained, when pumped with a peak power of 588 mW. Simulated results indicate that the time-delay experienced by the pulse can be tuned with the pump power and structural parameter of As_2Se_3 Rib Waveguide.

Key words: Single-mode waveguide, Intermodal dispersion, nonlinear optics, stimulated Brillouin scattering, Effective mode area, confinement loss.

LIST OF RESEARCH PUBLICATIONS

Journal

1. **Himanshu Pandey**, Than Singh Saini, Ajeet Kumar, "Design and Analysis of Highly Nonlinear Rib Waveguide Structure for the Generation of Slow Light", Fibre and integrated optics, 2016. (Communicated)

Conference

1. **Himanshu Pandey**, Than Singh Saini, Ajeet Kumar, "Design and Analysis of Trench-assisted Leaky Channel Waveguide for High Power Applications", ***AIP Conference Proc***., International Conference on Condensed Matter and Applied Physics, 30-31 Oct 2015, Govt. Engineering College Bikaner, Rajasthan, India, 1728, 020376, 2016; doi:10.1063/1.4946427.
2. **Himanshu Pandey**, Than Singh Saini, Ajeet Kumar, "Design and Analysis of Highly Nonlinear Rib Waveguide Structure for the Generation of Slow Light", Conf. Proceedings. ***OSA Young Student Congress***, 16-17 April, MNIT Jaipur, Rajasthan, India, OSA_YSC_114, (38-40), 2016.

ACKNOWLEDGEMENT

I take this opportunity as a privilege to thank all individuals without whose support and guidance, I could not have completed my project successfully in this stipulated period of time.

First and foremost I would like to express my deepest gratitude to my supervisor **Dr. Ajeet Kumar**, Asst. Professor, Department of Applied Physics, for his invaluable support, Patient guidance, motivation and encouragement throughout the period this work was carried out. I would like to thank **Than Singh Saini**, Research Scholar, for valuable time and interest in this project. I am grateful to both for closely monitoring my progress and providing me with timely and important advice, their valued suggestions and inputs during the course of the project work.

I am deeply grateful to **Prof. S.C. Sharma**, H.O.D. (Deptt. of Applied Physics) for his support for providing best educational facilities.

I also wish to express my heart full thanks to the classmates as well as staff at Department of Applied Physics of Delhi Technological University for their goodwill and support that helped me a lot in successful completion of this project.

Finally, I want to thank my parents, brother and friends for always believing in my abilities and for always showering their invaluable love and support.

Himanshu Pandey
M.Tech. NST
2K14/NST/03

CONTENTS

LIST OF FIGURES

LIST OF TABLES

CHAPTER 1

INTRODUCTION

1.1 Thesis Approach:

This thesis consists of a theoretical appraisal of a promising design of Stair-case leaky channel waveguide for high power applications and a highly nonlinear As_2Se_3 based Chalcogenide waveguide is reported for generation of tunable slow-light and its application at 1550 nm. Stair-case channel waveguide consists of multi-trench design that supports an effective single guided mode. This waveguide works on the principle of higher order mode discrimination. The cladding of waveguide is formed by alternate low and high index regions, which helps leaking out of higher-order modes while retaining the fundamental mode over the entire length of the waveguide. Slow-light refers to the possibility of controlling the group velocity of an optical signal, which can be achieved by modifying the dispersion of the medium or by designing the guiding structure. In this thesis, slow-light generation is carried out by designing Chalcogenide rib waveguide which has a structure similar to that of a strip or ridge waveguide, but the only difference is the strip has the same index as the high index planar layer beneath it and is part of the waveguiding core. Both the structure i.e. Stair-case large-mode-area waveguide and chalcogenide rib waveguide is put forward and analyzed in 'Comsol-Multiphysics' software, which solves complex electromagnetic fields using Finite-element method and hence, the confinement loss and effective-mode-area for fundamental mode is calculated along with the parameters of slow-light.

1.2 Thesis Objective:

The main objectives of the thesis are given as follows:

- Study of the fundamentals of optical waveguide, basic types of non-planar waveguides and its application in optical communication systems.
- Study the basics of nonlinear effects in optical fibres.
- Study of the basic methods to achieve slow-light and SBS based slow-light.

- Study the basics of various numerical methods which are used to model optical waveguides, like Finite-Element Method, Finite-Difference Method, Variational Method, Method of Moments.
- Design and analysis of Stair-Case Large-Mode-Area Leaky Channel Waveguide for High Power Applications.
- Design and analysis of highly nonlinear Chalcogenide Rib waveguide for slow-light generation.

1.3 Thesis Organization:

The detail of the work carried out in this project is organized in six chapters. Chapter 1 consists of an introduction, overview and objectives of the thesis. A literature review of topic such as basics of optical waveguide, slow-light and its mechanism, as well as its various applications in novel fields are explained in chapter 2. In chapter 3, a brief description of different modeling methods of the optical waveguide is given. Chapter 4 is related with design and analysis of stair-case large-mode-area Leaky channel waveguide and its applications for high powered devices. Chapter 5 consists of Design and analysis of nonlinear Chalcogenide Rib waveguide for slow-light generation. In chapter 6, the work carried out is concluded with scope for future work that can be done in this area.

CHAPTER 2

OPTICAL WAVEGUIDE AND SLOW-LIGHT

2.1 Optical waveguide and its classification:

An optical waveguide is a physical construction that provides passage to electromagnetic waves in the optical spectrum. It works on the principle of Total Internal Reflection (TIR). TIR is an optical phenomenon which occurs when a light wave strikes a boundary between two media at an angle greater than the critical angle (measured with respect to the normal to the surface). When light crosses a boundary of two materials with different refractive indices, a portion of the light refracts and propagates in the other medium and another portion reflects into the same medium. When the angle of incidence of the light at the boundary with respect to the normal of the surface increases, the refracted portion of the light decreases and at a certain angle, called the critical angle, the light travels along the boundary. Optical waveguides have many advantages over electrical transmission systems: greater channel capacity, lower losses, immunity to interference, and secure transmission [1]. Common types of optical waveguides include optical fibre and rectangular waveguides. Optical waveguides are used as components in integrated optical circuits or as the transmission medium in local and long haul optical communication systems. Optical waveguides can be classified according to their geometry (planar strip, or fibre waveguides), mode structure (single mode, multi-mode), refractive index distribution (step, or gradient index) and material (glass, polymer, and semiconductor).

Non-planar and planar waveguides

There are mainly two types of waveguides:

- In a **non-planar waveguide** of two-dimensional transverse optical confinement, the core is surrounded by cladding in all transverse directions, and n(x, y) is a function of both x and y coordinates. E.g. the channel waveguides and the optical fibres
- In a **planar waveguide** that has optical confinement in only one transverse direction, the core is sandwiched between cladding layers in only one direction, say the x

direction, with an index profile n(x). The core of a planar waveguide is also called the film, while the upper and lower cladding layers are called the cover and substrate.

Channel waveguides

The waveguides which are used in device applications are mostly non-planar waveguides. For a non-planar waveguides, the index profile n(x, y) is a function of both transverse coordinates x and y. There are different types of non-planar waveguides that are differentiated by the distinctive features of their index profiles. One very unique group is the circular optical fibres. Another important group of non-planar waveguide is the channel waveguides which assimilate:

- The buried channel waveguides
- The strip-loaded waveguides
- The ridge waveguides
- The rib waveguides
- The diffused waveguides

A **buried channel waveguide** consisting of a high-index waveguiding core buried in a low-index surrounding medium. The waveguiding core can have any cross-sectional geometry though it is often a rectangular shape.

A **strip-loaded waveguide** is developed by loading a planar waveguide, which already provides optical confinement in the x direction, with a dielectric strip of index $n_3 < n_1$ or a metal strip to facilitate optical confinement in the y direction as shown in Fig. 2.1. The waveguiding core of a strip waveguide is the n_1 region under the loading strip, with its thickness 'd' determined by the thickness of the n_1 layer and its width w defined by the width of the loading strip.

A **ridge waveguide** has a similar structure just like a strip waveguides, but the strip, or the ridge, on top of its planar structure has a high index and is actually the waveguiding core. A ridge waveguide has strong optical confinement because it is localized on three sides by low-index air (or cladding material).

A **rib waveguide** has a structure similar to that of a strip or ridge waveguide, but the strip has the same index as the high index planar layer beneath it and is part of the waveguiding core. These four types of waveguides are usually termed rectangular waveguides with a thickness d

in the x direction and a width w in the y direction, though their shapes are normally not easily rectangular.

A **diffused waveguide** is crafted by creating a high-index region in a substrate through diffusion of dopants, such as $LiNbO_3$ waveguide with a core formed by Ti diffusion. Because of the diffusion process, the core boundaries in the substrate are not sharply defined. A diffused waveguide also has a thickness d defined by the diffusion depth of the dopant in the x direction and a width w defined by the distribution of the dopant in the y direction.

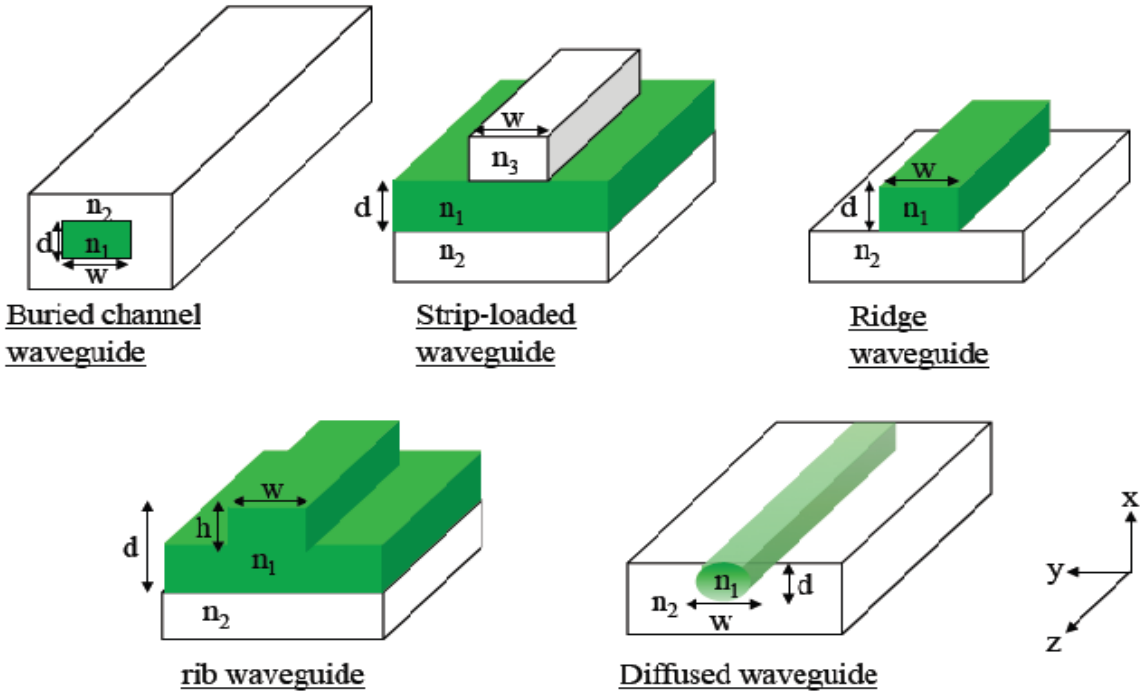

Fig. 2.1: Schematic representation of different types of optical waveguides.

One unique property of non-planar dielectric waveguides when compared with planar waveguides is that a non-planar waveguide supports hybrid modes in addition to TE modes and TM modes, whereas a planar waveguide supports only TE and TM modes. Except for those few revealing special geometric structures, such as circular optical fibres, non-planar dielectric waveguides generally do not have analytical solutions for their guided mode characteristics. Numerical methods, such as the beam propogation method, exist for analysing such waveguides.

2.2 Investigation of Channel waveguides:

The investigation and inspection of a channel waveguide is generally a convoluted task, and various approaches are used for ridge and channel guides. Since the index changes concerned in the former are so large, a TEM model cannot be used, and a rigorous solution is normally required. Fig. 2.2 shows one possible model of a ridge guide, which consists of a region of dielectric of rectangular cross-section localised by regions of different indices.

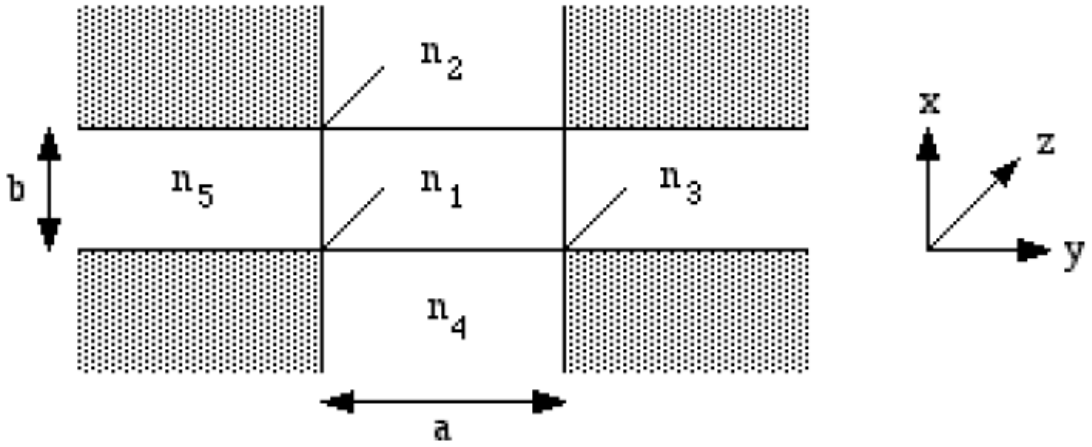

Fig. 2.2: Model of a rectangular dielectric waveguide (source: R.R.A. Syms and J.R. Cozens, Optical Guided Waves and Devices, chapter 9, page 5)

It has been shown that modes of such a guide can be found (at least approximately) by assuming solutions for the transverse variation of the electric field in the form of a product, i.e. as $ET(x, y) = E_1(x)\, E_2(y)$. Since the layers are individually uniform, we may guess that $E_1(x)$ and $E_2(y)$ must have the form either of cosinusoidal or of exponential functions, by analogy with the solution for a slab guide. These solutions are then built up in a piecewise function fashion, as follows:

- In region 1, the field is assumed to vary cosinusoidally with both x and y.
- In region 2, the field is assumed to decay exponentially with x, and vary cosinusoidally with y.
- In region 3, the field is assumed to vary cosinusoidally with x, and decay exponentially with y.

And so on. These fields are matched rigorously at the interfaces between Regions 1 and 2, 1 and 3, 1 and 4, and 1 and 5, but only approximately in the shaded corner regions. The result is a set of two-dimensional mode patterns, which are neither truly TE nor truly TM.

2.3 Rib waveguide and condition for single mode:

Rib waveguide have been analysed comprehensively over the years since they are oftenly used for lasers, amplifiers, modulators, and switches as integral parts to deliver photons and provide host medium to light matter interaction. The rib waveguide basically consists of three parts; a silica substrate, a thin layer on top of the substrate and a rectangular rib part. The index of the rectangular regions must be larger than the surrounding medium for the rib in order to guide light. Even though this fundamental waveguide configuration is very standard, there are attempts to modify the basic structure to confine light at low index medium.

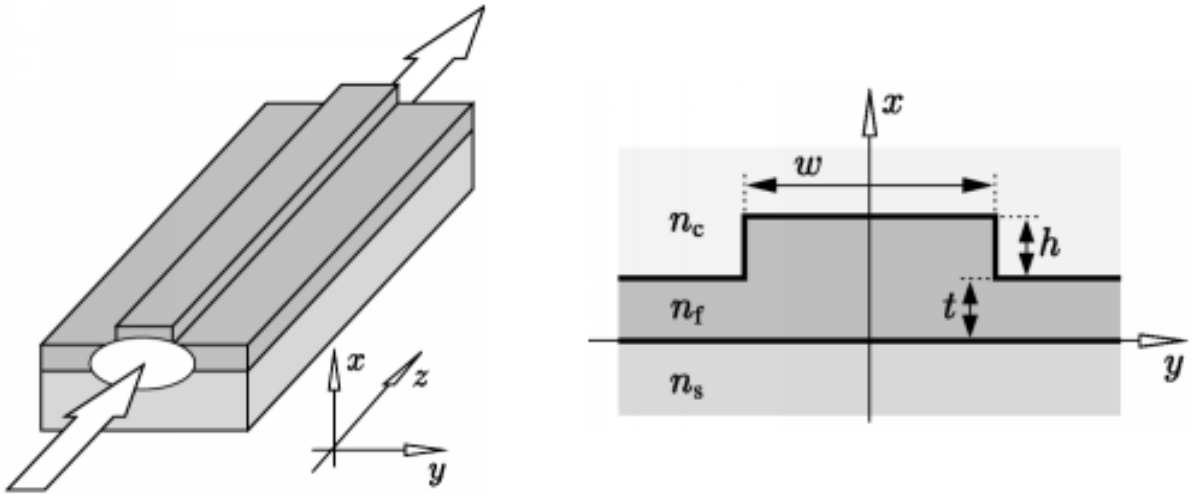

Fig. 2.3: Cross sectional view of rib waveguide and how light propagates in it

The principle of the confinement in the low index medium relies on the electric field discontinuity at the interface between high-index contrast materials. The low index medium is generally chosen as air, which makes it possible to carry high intensity light sources in air or to alleviate sensitive light interaction with the infiltrated material for sensing applications. By adding vertical, horizontal or cross type air slots, one can change the field confinement mechanism and also the polarization type of the rib waveguide. Lastly, polarization mode control and dispersion management are also very important in photonic integrated circuits.

2.3.1 Single Mode condition for rib waveguides:

Rib waveguides are used for the fabrication of important passive elements in integrated optics. When used in optical communication systems, care should be taken to ensure single mode propogation for their further coupling with single mode fibres. Single mode propogation is an important requirement for optical waveguide devices for use single mode fibre. It was first shown by Petermann using a mode matching technique, that rib waveguide of a large cross-section area (compared to wavelength) can have single mode behaviour.

Later this was applied by Soref *et al.* [2] to silicon rib waveguides with vertical sides. Equation (1) and (2) were claimed to give the conditions required for single mode behaviour.

$$\frac{W}{H} \leq \alpha + \frac{\frac{h}{H}}{\sqrt{1-\left(\frac{h}{H}\right)^2}} \qquad (2.1)$$

$$\frac{h}{H} \geq 0.5 \qquad (2.2)$$

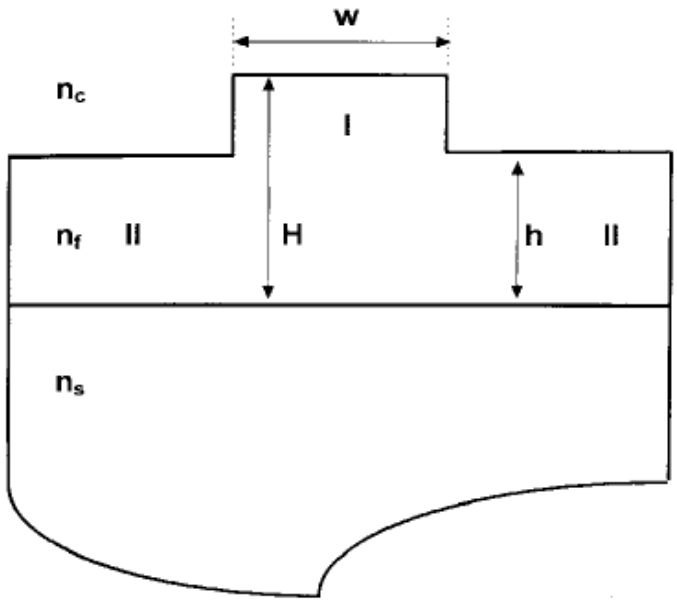

Fig. 2.4: Schematic diagram of rib waveguide (source: Souren P. Poggossian et al. Journal of lightwave technology, vol. 16, no. 10, October 1998)

As shown in Fig. 2.4, H is total of rib height, h is slab height, and W is the rib width. α is dimensionless constant, given in [1] as 0.3. Equation (2) arises from the need to be single mode in the vertical sense. If $\frac{h}{H} \geq 0.5$, any mode with two or more maxima vertically will be leaky, because the bottom maxima will couple to the fundamental mode of the surrounding slab. The problem was further analysed by Pogossian *et al.* [3] using the effective index method and a formulation previously used for single mode condition for silica waveguides. The result was same as (1) and (2) but with α=0, which agreed more favourably with experimental data from [4]. However it has also been claimed [2], that the effective large method is not suitable to predict single mode behaviour for rib waveguide which support more than one mode in slab region.

2.4 The Nonlinear Effects in Optical Fibre:

The conception of nonlinear effect in optical fibre is due to ultrafast third-order susceptibility χ^3. These effects in optical fibre occur mainly due to intensity reliance of refractive index of the medium or due to inelastic-scattering phenomenon. The nonlinear effects in optical fibre are due to the inelastic-scattering to a lower energy photon. The energy difference is absorbed by the molecular vibrations or phonons in the medium. In other words, one can state that the energy of a light wave is transferred to another wave, which is at a higher wavelength (lower energy) such that the energy difference appears in form of phonons. The term linear and nonlinear in optics, means intensity-independent and intensity-dependent phenomena respectively. Nonlinear effects in optical fibres [5] i.e. shown below, occurs due to (1) change in refractive index of the medium with optical intensity and, (2) inelastic scattering phenomenon.. Depending upon the type of input-signal, it manifests itself into three different effects such as Self-Phase Modulation (SPM), Cross-Phase Modulation (CPM), and Four-Wave Mixing (FWM). At high power level, the inelastic scattering phenomenon can induce stimulated effects such as Stimulated Brillouin-Scattering (SBS) and Stimulated Raman-Scattering (SRS). The intensity of scattered light grows exponentially if the incident power exceeds a certain threshold value. The difference between Brillouin and Raman scattering is that the Brillouin generated phonons (acoustic) are coherent and give rise to macroscopic acoustic wave in the fibre, while in Raman scattering the phonons (optical) are incoherent and no macroscopic wave is generated.

The nonlinear effects depend on transmission length. The longer the fibre link length, the more will be the light interaction and greater the nonlinear effect. The effective link length is obtained as

$$L_{eff} = \frac{(1 - \exp(-\alpha z)}{\alpha} \qquad (2.3)$$

Where α is coefficient of attenuation.

The effect of nonlinearity grows with intensity in fibre and the intensity is inversely proportional to area of the core. The A_{eff} is related to the actual area (A) and the cross-sectional distribution of intensity $I(r,\theta)$ as

$$A_{eff} = \left[\frac{\iint r\ dr\ d\theta\ I(r,\theta)}{\iint r\ dr\ \ d\theta I^2(r,\theta)}\right] \qquad (2.4)$$

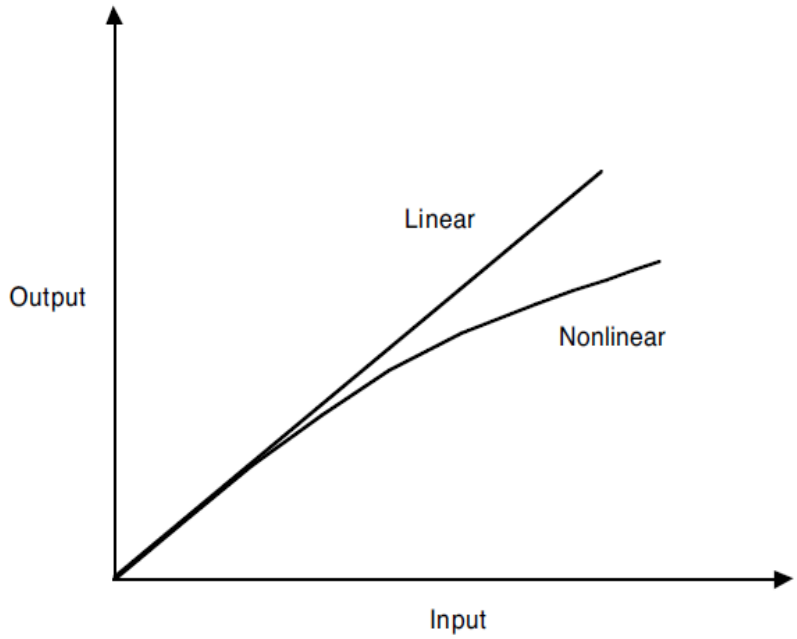

Fig. 2.5: Graph depicting Linear and nonlinear interactions

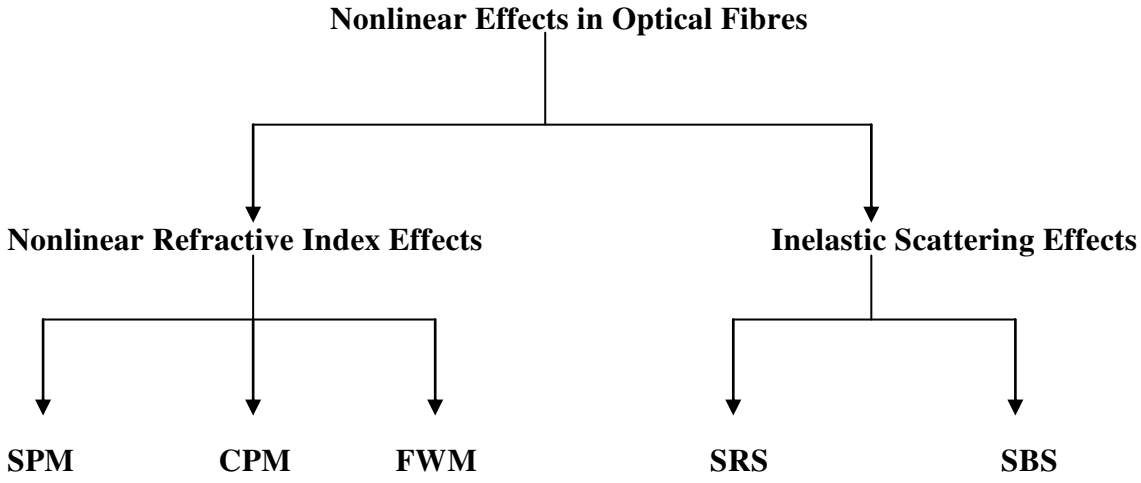

Except for SPM and CPM, all nonlinear effects provide gains to some channel at the expense of depleting power from other channels. SPM and CPM affect only the phase of signals and can cause spectral broadening, which leads to increased dispersion. Due to the following, the nonlinear effects in optical fibres are an area of academic research [5].

- Use of in-line optical amplifier has resulted in a substantial increase in absolute value of the power carried by a fibre.
- Use of single mode fibre (SMF), with small cross section of light-carrying area has led to increased power intensity inside the fibre.

- The implementation of high-bit-rate (>10 G bits/s per channel) systems.
- The implementation of multi-wavelength systems together with optical amplifier.

2.5 Overview and Introduction of Slow-light:

The group velocity of light pulses in optical media can become significantly slower and even faster, than the expected speed of light. These phenomenons are known as slow and fast light. The light travels in vacuum at a very high velocity given by *c*, which is approximately 3×10^8 m/sec. The advantage of this ultrahigh speed of light is that the data transmission between two points whether they are separated on global scale or on a single chip, becomes efficient. While these light are efficient but there is a problem in controlling these lights in time domain. Hence there is a requirement of "slow-light" to overcome this problem.

Slow-light means the feasibility of modulating the group velocity of an optical pulse, which can be realized by reforming the dispersion of the medium or by designing the guiding structure. It is basically the propogation of optical pulse or other modulation of an optical carrier at a very low group velocity. When light propagates through a material, it travels slower than the vacuum speed, *c*. This is a change in the phase velocity of the light and is manifested in physical effects such as refraction. This reduction in speed is quantified by the ratio between c and the phase velocity. This ratio is called the refractive index of the material. Slow-light is a dramatic reduction in the group velocity of light, not the phase velocity. We denote the group velocity by $v_g = {}^{c}/_{n_g}$, where, *c* is the speed of light in vacuum and n_g is known as the group index. The group velocity depends not only on the refractive index of the material, but also the way in which the refractive index changes with frequency [7]. If the dispersion relation of the refractive index is such that the index changes rapidly over a small range of frequencies, then the group velocity might be very low, thousands or millions of times less than *c*, even though the index of refraction is still a typical value (between 1.5 and 3.5 for glasses and semiconductors). Slow-light is an important area of research that is of fundamental interest and has great potential for applications. The use of optical waveguides is particularly attractive for application since it can be readily integrated with existing technologies.

The technique based on slow-light provides the hopeful solutions of the broadband and tunable time-delay for microwave and millimetre wave systems. By controlling and storing the light and enhancing nonlinearity, it is possible to design on-chip all-optical signal processing photonic crystal devices. When one allows light to interact with an optically

resonant media, it is possible to control the speed of light and its other propogation characteristics. In the field of microwave-photonics (MWP) in which photonics is exploited to process microwave signals, breakthrough progress has been demonstrated [6]. In MWP, Slow-light enables a continuous tuning of the phase-shift or time delay of the microwave signals that modulate the optical carrier, with very low losses and distortion and over bandwidths that can be incomparably larger than those provided by electronic devices of comparable cost. As for photonics, the striking property of structural slow-light to enhance optical nonlinearities is playing a major role in the progress toward on-chip, all-optical signal processing.

2.6 Mechanisms to achieve Slow-light:

Many approaches have been proposed and demonstrated to achieve slow-light. Basically, these mainly falls into one of two general categories, namely, "microscopic" and "macroscopic" slow-light.

Microscopic mainly signifies to those processes in which the variation of group index is mainly due to influence of light-matter at the atom/molecule level. A slow-light medium typically indicates that n_g can be very different than n, i.e., the magnitude of $\omega(^{\partial n}/_{\partial \omega})$ term is an appreciable quantity. Major examples of microscopic slow-light include electromagnetically induced transparency (EIT), coherent population oscillations (CPO), naturally occurring resonance or band edge, stimulated Brillouin scattering (SBS), stimulated Raman scattering (SRS), spectral hole burning, parametric amplification, and so on.

Secondly, macroscopic slow-light, indicates that the manipulation of the "effective group velocity" of light in the medium is achieved through the interaction between light and the structural geometry of an element that is comparable or larger than the optical wavelength. A macroscopic slow-light element is typically not spatially homogeneous but has a structural geometry with characteristic feature size which is similar or very large, when compared to wavelength. Macroscopic slow-light incorporates photonic band gap structures, single and coupled ring resonator, fibre or waveguide grating structures.

In such cases, the slow-light effect is best described by the group delay of propagation through the entire element, or at least one period of the structure if it is periodic, as follows,

$$\tau_g = \frac{\partial \emptyset(\omega)}{\partial \omega} \qquad (2.5)$$

Where $\emptyset(\omega)$ is the phase of the complex transfer function$\hat{H}(\omega) = A(\omega)exp[i\emptyset(\omega)]$. It is also convenient to define the effective refractive index n_{eff} and effective group index $n_{g,eff}$ by assuming that the medium is homogeneous;

$$n_{eff}(\omega) = \frac{\emptyset(\omega)c}{\omega L} \qquad (2.6)$$

$$n_{g,eff} = n_{eff} + \omega\frac{\partial n_{eff}}{\partial \omega} \qquad (2.7)$$

Where c is the speed of light in vacuum, and L is the length of the element or a period of the element.

2.6.1 Theory of SBS:

When highly severe pump wave interacts with the counter propagating, weak signal wave, then a slowly travelling wave is generated. This creates travelling density variations (*i.e.* acoustic wave) in the medium. Consequently, acoustic wave leads to a travelling grating of refractive index variation in the medium. When narrow-band laser radiations transmitted inside an optical waveguide, some of the incident light scatters backward due to the nonlinear process called stimulated Brillouin scattering (SBS). This scattering creates disturbance for some nonlinear signal processing applications that involve using a strong continuous wave (CW) pump. When phase matching condition is satisfied, the travelling refractive index grating can couple optical power in between pump and signal waves, when the frequency difference between the pump and the signal power is equal to Brillouin frequency shift (Ω_B). It gives rise to Ω_B . So,

$$\Omega_B = \omega_P - \omega_S, K_A = K_P - K_S \qquad (2.8)$$

Where, ω_P is the frequency of pump wave and ω_S is the frequency of the stoke wave and $K_P$and K_S are the wave vectors of the pump and stoke waves respectively.

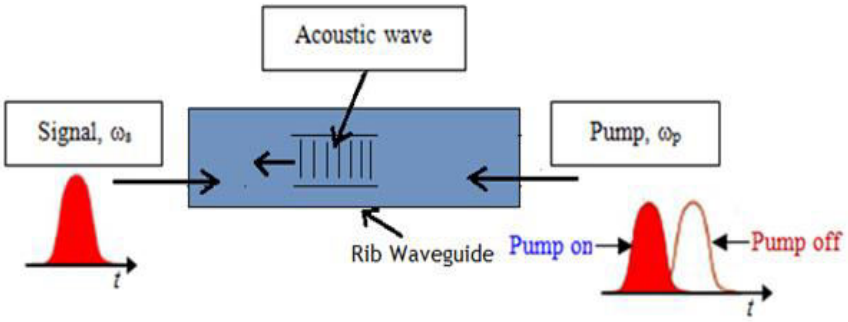

Fig. 2.6: Schematic of the principle of stimulated Brillouin scattering in rib waveguide

If I_P be the pump intensity, I_S be stokes wave intensity, $g_B$the Brillouin gain coefficient and α_P and α_S be the fibre losses at the pump and stokes frequencies then the coupled nonlinear differential equation for pump and signal waves can be given as follows [7].

$$\frac{dI_P}{dZ} = -g_B I_P I_S - \alpha I_P \qquad (2.9)$$

$$-\frac{dI_S}{dZ} = +g_B I_P I_S - \alpha I_S \qquad (2.10)$$

If the fibre losses are zero i.e. α = 0 then $\frac{d(I_p - I_S)}{dZ} = 0$ and $(I_P - I_s)$ remains constant along the fibre. Let the pump wave is undepleted so using the equations

$$I_P(Z) = I_P(0)e^{-\alpha z} \qquad (2.11)$$

We can solve the above equations and the solution is given as

$$I_S(0) = I_s(L)\exp[\left(\frac{g_B P_0 L_{eff}}{A_{eff}}\right) - \alpha L] \qquad (2.12)$$

where, A_{eff} is the effective mode area of the waveguide, P_0 is the input pump power and can be given as $P_0 = I_P(0) * A_{eff}$, α is the loss in the waveguide, L is the real length of the waveguide and L_{eff} is the effective length of the waveguide which can be calculated using the formula.

$$\text{Leff} = \frac{[1 - \exp(-\alpha L)]}{\alpha} \qquad (2.13)$$

Where, L is the real length and L_{eff} is the effective length of the waveguide, α is the attenuation constant for the waveguide.

In the basic model of SBS, the integrating between two counter propagating optical waves and a longitudinal wave, this plays the pivotal role in the wave interaction. When two optical wave having frequency difference equal to the frequency of the acoustic wave, the interaction will efficiently lead to the formation of a dynamic Bragg in the core of a waveguide which can diffract the light from the higher frequency wave back into the lower frequency wave. As a result the signal wave will experience a gain [8-10].

The Brillouin gain can be expressed as

$$g_B(\Omega) = \frac{g_p \left(\frac{\Gamma_B}{2}\right)^2}{[(\Omega - \Omega_B)^2 + (\Gamma_B/2)^2]} \qquad (2.14)$$

Where, g_p is the peak value of the Brillouin gain at $\Omega = \Omega_B$ and given by the relation

$$g_P = g_B(\Omega_B) = \text{gB} = \frac{2\pi n^7 {p_{12}}^2}{c{\lambda_P}^2 \nu_A \rho_0 \Gamma_B} \qquad (2.15)$$

Here, ρ_0 is the density and $p_{12}$is the longitudinal elasto-optic coefficient. The full width at half maximum (FWHM) of the gain spectrum is related to Γ_B by the relation$\Delta\, \nu_B = \Gamma_B/(2\pi)$; , Γ_B is the Brillouin line width and defined by $\Gamma_B = \tau_{photon}^{-1}$, where τ_{phonon} is the phonon life time in the material [11].

The effective mode area A_{eff} of the propagating mode is given as

$$A_{eff} = \frac{\left(\iint_{-\infty}^{\infty} |E|^2 dx\, dy\right)^2}{\left(\int_{-\infty}^{\infty} |E|^4\, dx\, dy\right)} \qquad (2.16)$$

Where, E is the electric field distribution inside the PCF core.

The Brillouin gain coefficient of PCF can be calculated using the relation [10]

$$G = 10 \log\left[exp\left(\frac{g_B P_0 L_{eff}}{A_{eff}}\right) - \alpha L\right] \qquad (2.17)$$

Where P_0 the pump power and K denotes the polarization factor and depends on the polarization properties of the waveguide. The value of Polarization factor is 1 if the polarization is maintained and it is 0.5 if polarization is not maintained. Although, some results [11, 8, and 9] showed that K = 0.667 is more appropriate, for waveguide which is low-

birefringence and very high polarization beat length. In our simulation K = 0.667 has been used.

The maximum allowable pump powerP_{max} (the maximum pump power above which the output pulse get distorted), related to the Brillouin gain coefficient g_B by the following relation [11, 12]

$$P_{max} = 21 \frac{A_{eff}}{K\, g_B\, L_{eff}} \qquad (2.18)$$

Where,A_{eff} is the effective cross-sectional area. Once pump power approached to P_{max} then the backscattered wave can be generated from the background noise in the fibre, which leads to serious output pulse distortion. Therefore, the value of pump power must be smaller than the P_{max}.

The minimum value of pump power which is required to initiate the SBS effect is given by

$$P_{min} = \frac{\alpha\, A_{eff}\, L}{K\, g_B\, L_{eff}} \qquad (2.19)$$

The SBS-induced time delay per unit length and per unit pump power by slow-light devices can be expressed as [7, 13]

$$\frac{\Delta t_d}{L_{eff}} = \frac{P_p\, g_0\, K}{\Gamma_B} \qquad (2.20)$$

Figure of Merit (FOM) of the waveguide can be represented as

$$FOM = 4.34\left(\frac{g_B K L_{eff}}{A_{eff} n L}\right) \qquad (2.21)$$

Main applications of SBS phenomenon which are suitable for making many optical devices are Fibre sensors, Brillouin fibre amplifier, Beam combiner, Pulse delaying and advancement, and Pipeline buckling detection.

2.6.2 Applications and Practical considerations of slow-light:

Besides the property of "decelerating" light pulses or optical wave packets, slow-light has many other fundamental properties that can lead to other applications and its utilisation [9]. One of such properties is that the refractive index of a slow-light medium is highly frequency dependent. In other words, a small shift in frequency $\delta\omega$ will cause a large change in the wave number δk inside a slow-light medium. This is very integral to the spectroscopic

response of interferometric devices, and it is worthwhile to examine how the slow-light can enhance the performance of spectroscopic interferometers, both in ideal and practical cases. Alternatively, fast light can be used to build interferometers that are insensitive to wavelength drift. Such a "white-light" interferometer can be used for ultrahigh-precision metrology such as gravitational-wave detection.

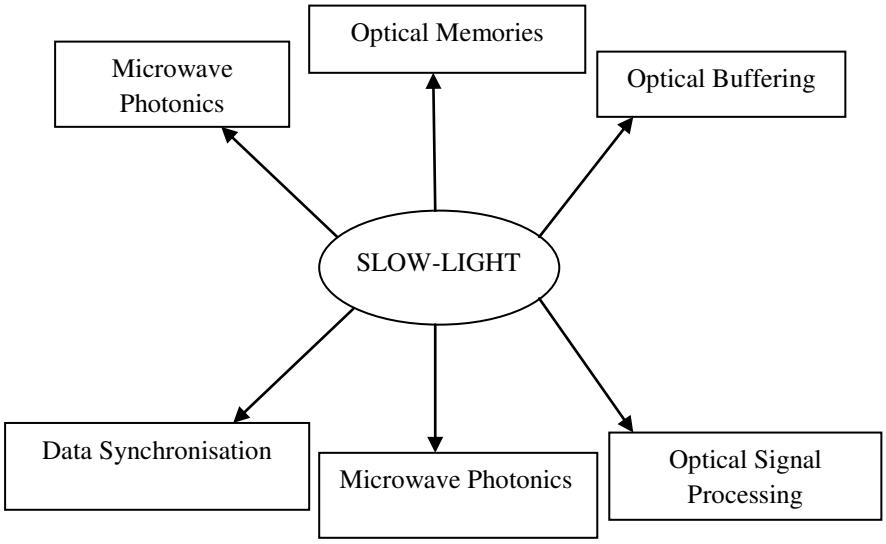

Fig. 2.7: Schematic diagram representing applications of Slow-light

Slow-light allow researchers to conduct many exciting fundamental studies of physics and light propagation, but they also have many potential practical applications. The applications proposed for slow-light cover many different areas, but they can be grouped into three main themes. Perhaps the most obvious use for a slow-light medium is as a tunable delay line, a compact device that can store or buffer light pulses for a time or perhaps even indefinitely. Tunable optical delay lines could fine a number of applications within telecommunication networks, as well as in optical coherence tomography (OCT), ultrafast pulse metrology, coupled cavities and various kinds of optical signal processing. Slow-light can also be used to enhance the nonlinear effects of an optical material, leading to smaller devices and lower operating power in applications that require a high degree of nonlinearity. Slow light has immense utilisation in nonlinear photonics, as it can highly enhance the nonlinearity. Finally, slow-light can enhance interferometry, producing more sensitive and more stable interferometers.

CHAPTER 3

MODELING METHODS FOR OPTICAL WAVEGUIDE

3.1 Introduction:

The modeling plays a very crucial role in design and analysis of optical waveguide. Numerical simulations perform major role in the waveguide designing as well as its modeling. Several approaches to modeling light transmission in various types of optical waveguide incorporates Beam propagation method (BPM), Finite element method (FEM), Finite difference time domain method (FDTM), Transfer matrix method (TMM), Multi-pole method, Moment method, Variational method. Strategically, there are two basic approaches to the numerical solution of a particular research problem. The first is the development of a homemade numerical code. The second approach relies on adaptation of commercial or freely available Computer Aided Design (CAD) tools. The advantage of developing homemade codes incorporates full access and control over the source code and therefore, flexibility with regard to code modification and improvement. On the other hand reliable ready-to-use CAD tools are applicable to a variety of different physical problems and could be optimized for speed, memory, usage and so forth. Therefore, these CAD tools are being widely utilized in industrial product development as well as in academic research. In this thesis, the proposed structure and the numerical studies presented mainly rely on solving the equations of electromagnetic waves propagation by using the finite element method technique (FEM) in COMSOL Multiphysics (version 4.2), a commercial software package.

3.2 Numerical Methods:

3.2.1 The Beam Propagation Method (BPM):

The beam propagation method (BPM) is a powerful technique that can be used to solve optical circuits where $\Delta << 1$. In this case, the modes are governed by the scalar Helmholtz equation [14]

$$\left[\Delta^2 + \frac{\omega^2}{c^2} n^2(\omega, x, y)\right] E = 0 \qquad (3.1)$$

Where

$$\Delta^2 = \frac{\partial^2}{\partial x^2} + \frac{\partial^2}{\partial y^2} + \frac{\partial^2}{\partial z^2} \qquad (3.2)$$

h is the height of the waveguide and E is the transverse component of the electric field as a function of the circular frequency ω and the dimensional coordinates $x, y \; and \; z$, whereas the refractive index is a function of $\omega, x \; and \; y$.

Describing E as

$$E(\omega, x, y, z) = \varepsilon(\omega, x, y, z) e^{-jkz} \qquad (3.3)$$

and substituting it into equation 3.1 yields

$$\frac{\partial^2 \varepsilon}{\partial x^2} + \frac{\partial^2 \varepsilon}{\partial y^2} + \frac{\partial^2 \varepsilon}{\partial z^2} - 2jk \frac{\partial \varepsilon}{\partial z} - k^2 \varepsilon + \frac{h^2}{c^2} n^2 \varepsilon = 0 \qquad (3.4)$$

Therefore

$$-\frac{\partial^2 \varepsilon}{\partial z^2} + 2jk_0 \frac{\partial \varepsilon}{\partial z} = \nabla_{\neg}^2 \varepsilon + k_0^2 \left\{ \left[\frac{n(x,y)}{n_0} \right]^2 - 1 \right\} \varepsilon \qquad (3.5)$$

Where $\nabla_{\neg}^2 = {\partial^2}/{\partial x^2} + {\partial^2}/{\partial y^2}$ and assuming $k^2 = {\omega^2}/{c}$. Neglecting the leftmost term in

equation 3.4 yields the well-known parabolic or paraxial approximation of the Helmholtz equation

$$2jk_0 \frac{\partial \varepsilon'}{\partial z} = \Delta_{\neg}^2 \varepsilon' + k_0^2 \left\{ \left[\frac{n(x,y)}{n_0} \right]^2 - 1 \right\} \varepsilon' \qquad (3.6)$$

The Eigen solutions of equation 3.5 and 3.6 can be expressed as

$$\varepsilon(x, y, z) = u(x, y) e^{-j\beta z} \qquad (3.7)$$

$$\varepsilon'(x, y, z) = u'(x, y) e^{-j\beta z} \qquad (3.8)$$

Substituting equations 3.7 and 3.8 back into equations 3.5 and 3.6 provides the relationship between the eigen values as

$$\beta = k_0 \left[1 - \left(1 + 2\frac{\beta'}{k_0} \right)^{1/2} \right] \qquad (3.9)$$

The conclusion from equations 3.9 is that eigen values can be obtained by solving the parabolic or Fresnel equation [14].

Equation 3.9 is solved numerically by using an implicit finite difference scheme. However, a fundamental physical limitation exists resulting from the parabolic approximation to the Helmholtz equation. The effect of these limitations can be relaxed by using more accurate approximations, such as Pade approximations found in the Beam PROP software.

3.2.2 Perturbation Method:

This method replaces the profile of n by an approximate profile defined by $n_{app}(x, y)$ for which the analytical solution to the wave equation can be obtained. If the approximate refractive index is very close to the actual refractive index, the analytical result will be very close to the true wave equation solution. Based on the completeness of modes, the true wave mode can be expressed approximately in terms of the superposition of the complete set of analytical solutions. The perturbation expressions can be applied to waveguides of an arbitrary cross-section, and the integration only needs to be carried out over the regions of interest where the approximate index profiles are different from the actual ones.

3.2.3 Moments Method:

The method of moments (MOM) is a general procedure for solving the inhomogeneous equation $L\emptyset = g$ where L is an operator which may be differential, integral, or integro-differential, g is the known excitation or source function, and $\emptyset$ is the unknown function to be determined. The method owes its name to the process of taking moments by multiplying with appropriate weighing functions and integrating. The use of MOM in EM has become popular since the work of Richmond in 1965 and Harrington in 1967. The method has been successfully applied to a wide variety of EM problems of practical interest such as radiation due to thin-wire elements and arrays, scattering problems, analysis of micro strips and lossy structures, propagation over an inhomogeneous earth, and antenna beam pattern.

3.2.4 Finite Element Method:

The Finite element method (FEM) has its origin in the field of structural analysis. Although the finite difference method (FDM) and the method of moments (MOM) are conceptually simpler and easier to program than FEM. FEM is a more powerful and versatile numerical technique for handling problems involving complex geometries and inhomogeneous media. The systematic generality of the method makes it possible to construct general-purpose computer programs for solving a wide range of problems. Due to its flexibility and versatility,

the finite element method has become a powerful tool throughout engineering disciplines. It has been applied with great success to numerous EM–related problems. Such application incorporates transmission line problems, optical and microwave waveguide problems, electric machines, scattering problems, human exposition to EM radiation.

The finite element analysis of any problem involves basically four steps [15]:

- Discretizing the solution region into a finite number of sub regions or elements,
- Deriving governing equations for a typical element,
- Assembling of all elements in the solution region, and
- Solving the system of equations obtained.

The further explanation and equations are given in chapter 4, section 4.3.

3.2.5 Finite Difference Time Domain Method:

The finite-difference time-domain (FDTD) formulation of EM field problems is a convenient tool for solving scattering problems. The FDTD method, first introduced by Yee [16] in 1996 and later developed by Taflove is a direct solution of Maxwell's time-dependent curl equations. The scheme treats the irradiation of the scatterer as an initial value problem. It is a versatile modeling technique used to solve Maxwell's equations, since it calculates the E and H fields everywhere in the computational domain. A wide variety of linear and nonlinear dielectric and magnetic material can be easily modeled. Major drawbacks are high time consuming and memory complexity of the algorithm

3.2.6 Boundary-Element Method:

Boundary Element Method (BEM) is basically used for solving two dimensional optical waveguide problems. BEM requires integration along the boundary only. It has been shown that they are modeled with high accuracy and very precisely. Many special optical waveguide like PCFs are studied and analyzed using BEM. As it requires the integration along the boundary only. This indicates that meshing is mainly simple for two-dimensional problems. In BEM high accuracy is achieved with very few numbers of unknown. The advantage of BEM is that the external boundary conditions are not desired for open boundary. The major limitation is its time consuming process.

3.3 Effective Index Method:

The effective index method, developed by Hocker and Burns in 1977, converts a two dimensional waveguide to two orthogonal oriented one-dimensional waveguides with direct interaction. Here a general rectangular waveguide is decomposed into orthogonal-oriented slab waveguides. The horizontal slab maintains the same core index, whereas the vertical slab waveguide is solved by replacing the core index of refraction by the effective index defined by $n_{eff} = \beta_s/k_0$ (with β_s denoting the propagation constant of the slab waveguide). The procedure is to solve the characteristic wave equation for the TE and TM modes of the horizontal section. Once β_s is found, n_{eff} is calculated and used as the core index of the vertical waveguide section. From this the approximate propagation constant of the rectangular waveguide is calculated through the characteristics wave equation describing the vertical waveguide section.

CHAPTER 4

DESIGN AND ANALYSIS OF STAIR-CASE LARGE-MODE-AREA LEAKY CHANNEL WAVEGUIDE FOR HIGH POWER APPLICATIONS

4.1 Introduction:

Integrated optic waveguide lasers have been a matter of significant attention for research in the last few decades, because of their unique features such as compactness and possibility of integration [17-22]. Single mode (SM) waveguides are usually employed in such lasers to avoid mode competition and intermodal dispersion. Single mode operation also ensures good beam quality, which is indispensible for engineering applications, especially when the laser is coupled to a single mode optical fibre. Considerable methods have already been implemented to improve and enhance the output power of waveguide laser. A conventional optical waveguide requires a small core area to provide single mode operation, where the tight confinement can reduce the optical damage threshold and at the same time, give rise to significant unwanted nonlinear optical effects including four wave mixing, cross phase modulation, stimulated Brillouin scattering (SBS), stimulated Raman scattering (SRS). The preferred waveguide structure for high-power applications should have a large and single mode core. In fact there have been attempts to increase the mode areas in fibers for applications in optical communications and high power lasers and amplifiers [23-26]. One can increase the effective mode area of a fibre by controlling the refractive index profile in the core or the refractive index difference between the core and the cladding [27-29]. A large mode area (LMA) fibers based on using azimuthally segmented cladding profiles which do not rely on area holes and can offer mode areas comparable to those of large core holey fibers. In Rectangular geometry, large core single mode waveguide for single mode operation have been achieved by using small index contrast in polymer waveguide and by deep etching in semiconductor waveguide [30-32]. The development of LMA waveguide is very important for a broad range of the practical applications most notably those requiring either the delivery or generation of high power optical beams [33-36]. Thus, an interesting research of

waveguide is the realization high power laser applications by means of endlessly single mode waveguide with large mode area. These properties provide scaling budding for waveguide laser and amplifier systems [18]. By using proficient pumping schemes, proper waveguide design, photonic crystal fiber dominated and acceptable rare earth metal like Scandium, Terbium, Holmium, Erbium etc for large core single mode operation, we can able to enhance the output power of waveguide laser.

The effective mode area of conventional optical waveguide can be expanded by increasing its core. However, when the core size is increased, the refractive index contrast between core and cladding must be reduced to achieve single mode operation. If the index contrast is not reduced, the waveguide become multimode which demean the quality of output beam. Various techniques such as modal discrimination which are needed to suppress the redundant higher order modes. Since the last two decade researchers have tried their level best to achieve LMA waveguide with SM operation for applications in densely fabricated optical devices and high power driven waveguide laser and amplifiers.

The following design is a stair-case leaky channel waveguide which works on the principle of mode filtering; High leakage loss to higher modes and nominal loss to fundamental mode fortify the LMA operation. The proposed design of LMA waveguide has been simulated using commercially available software 'COMSOL Multiphyiscs' based on finite element scheme. With suitable cladding parameters, proposed structure ensures extended SM operation in the spectral range of 1.25 – 2.0 μm with the rectangular core area as large as 50 μm^2. Such large core area waveguide structure is able to subdue unwanted nonlinear effects efficiently. Thus Proposed channel waveguide is suitable for high power delivery devices such as high power waveguide laser and amplifiers.

4.2 Design of the proposed channel waveguide:

Fig. 4.1 shows the transverse cross-sectional view of the proposed large core size channel waveguide structure which is featured by a rectangular core and a geometrically assisted multi-trench cladding in *y*-direction. The core has a refractive index n_1, thickness h_0 and width $2a$ is formed on a substrate with lower refractive index n_2. The region on each side of the core consists of low-index trenches of the depth h_1, h_2, h_3, h_4 in stair manner.

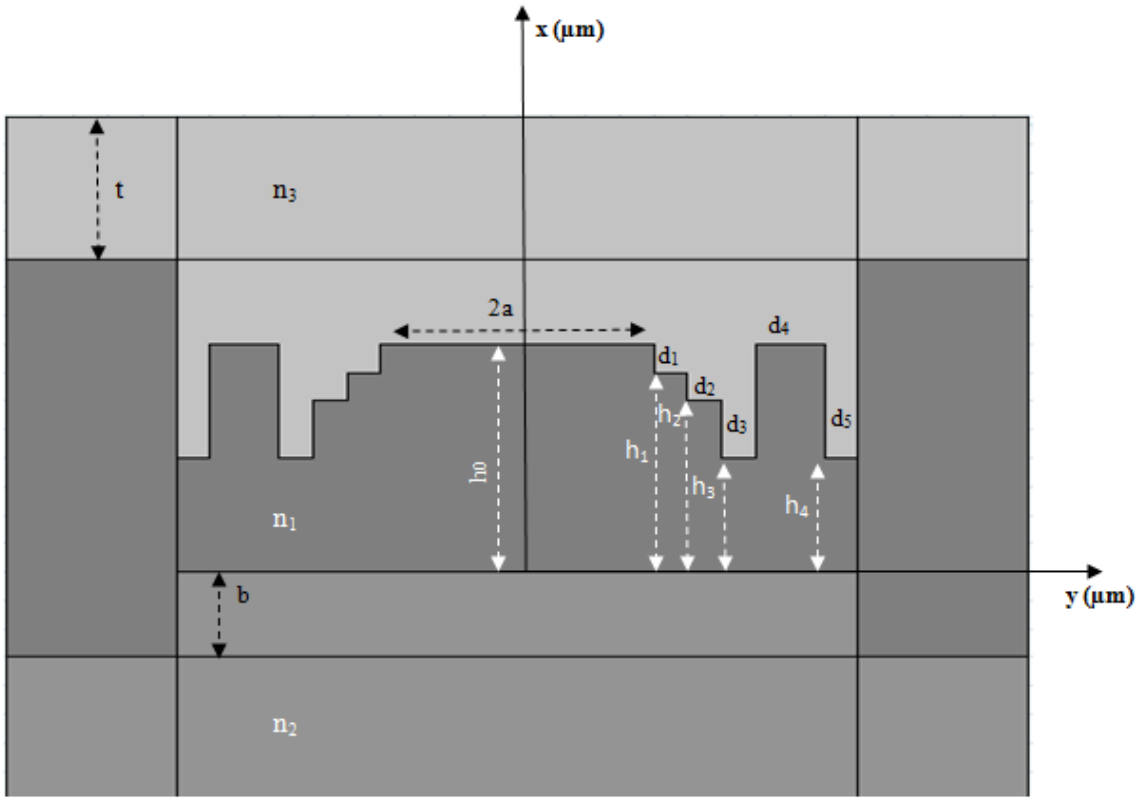

Fig. 4.1: Cross-sectional view of proposed multilayer leaky channel waveguide

The cladding is made by the same material as that of the core. The structure is covered by another lower index material of the refractive index n_3.We have inserted a perfectly matched layer (PML) around the waveguide structure of thickness t which is an artificial absorbing layer for wave equations, commonly used to truncate computational regions. It is constructed in such a way that there is no loss in the tangential direction to the interface between the lossless region and the PML. Here the role of the perfectly matched layer is to calculate accurate leakage losses of the modes propagating in the core of the proposed channel waveguide structure. This proposed multi-trench large core size channel waveguide can fabricated by the well known method known as reactive ion etching technique.

4.3 Method of Analysis:

The proposed waveguide is examined by the finite element method [15]. The PML boundary conditions are used to calculate accurate leakage losses of the modes propagating in the core of the proposed channel waveguide structure. The Maxwell vector equations for anisotropic PML is given by the following relation

$$\nabla \times ([s]^{-1} \nabla \times E) - k_0^2 \, \mathrm{n}^2 \, [\mathrm{s}] \, E = 0 \qquad (4.1)$$

$$[\mathrm{s}] = \begin{pmatrix} s_y/s_x & 0 & 0 \\ 0 & s_x/s_y & 0 \\ 0 & 0 & s_x \, s_y \end{pmatrix} \qquad (4.2)$$

Where, E is the electric field vector. $k_0 = 2\pi/\lambda$ is the wave number in the vacuum, and λ is the operating wavelength, n is the refractive index, [s] is the PML matrix, s_x and $s_y$are the PML parameters.

Propagation constants of the propagating modes are complex. The real part of the propagation constant gives the leakage loss of the mode. The leakage loss of the mode is determined by the imaginary part of the propagation constant using the following equation:

$$L\left(\frac{dB}{m}\right) = \frac{40\,\pi}{\ln(10)\lambda} lm\left(n_{eff}\right) = 80686 k_0 lm(n_{eff}) \qquad (4.3)$$

Where, Im (n_{eff}) is the imaginary part of propagation constant, λ is the free space wavelength in meter. In this work our aim is to increase the differential leakage loss between first higher order mode and fundamental mode keeping the leakage loss of fundamental mode in its acceptable range (< 1dB/mm). It is well known fact that, in general condition, the leakage loss of mode increases with mode order. It is therefore, sufficient to calculate the leakage losses of only first two modes in order to demonstrate the mode filtering.

4.4 Numerical Results and Discussion:

Numerical simulations have been implemented for the following parameters, n_1 = 1.5448, n_2 = 1.444, n_3= 1.512, t = 2 µm, λ = 1.55 µm. These parameters are typically of a polymer waveguide which is fabricated on silica substrate. All the simulating results illustrated in the Fig. 4.2 to Fig. 4.6 are performed at 1.55 µm wavelength. In order to choose the allowed operating range of parameters, the maximum loss for the x-polarized fundamental

(E_{11}^x) mode is set to 1.0 dB/mm while the minimum loss for first higher order (E_{21}^x) mode is set to 5.0 dB/mm. Thus, a waveguide of length less approximately 4 mm is utilised to show the effective SM operation.

By varying the different parameters, it is observed that the leakage losses of other higher modes are higher than that of E_{21}^x mode. Therefore, in order to achieve effective SM operation, it is sufficient to show the filtering of E_{21}^x mode from the waveguide. We have used the *x*-polarized fundamental and first higher order mode to illustrate the properties of the proposed channel waveguide. From Fig. 4.2 it is apparent that the leakage loss of E_{11}^x mode decreases linearly upto 2 µm wavelength and falls gently with increase in value of *a* and leakage loss of E_{21}^x mode also decreases with *a.* Here we have not considered the material absorption loss and surface roughness. Therefore leakage loss of higher order mode may be increased on adding absorption loss of the material. The effective area decreases upto a = 2 μm and beyond this value of *a*, (*i.e.* a > 3 µm) the effective area increases unexpectedly. We have obtained the high differential leakage loss which is desired for effective single mode operation of channel waveguide.

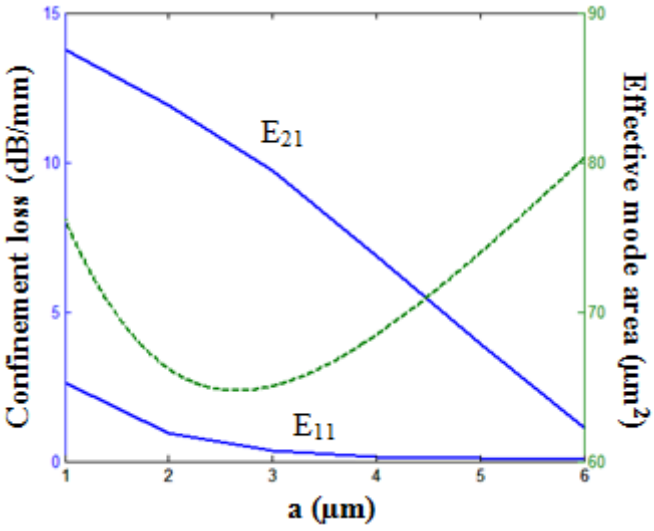

Fig. 4.2: Effect of core parameter an on leakage loss and effective mode area of first two modes of the waveguide at 1.55 µm wavelength when d_3 = 3 µm, h_3 = 5 µm, d_4 = 0.5 µm, h_4 = 7 µm.

Geometrically shaped cladding parameters (*i.e.* h_1, h_2, h_3, h_4, d_1, d_2, d_3 and d_4) which actually define the shape of multi-layered cladding are used to control the leakage losses of the modes. We have investigated the effect of d_3, d_4, h_3 and h_4 on single mode operation of the waveguide. Our study shows that these parameters have effective control on the leakage loss and can be used to design LMA SM channel waveguide. Beyond that these cladding parameters also give us freedom to further optimize the design for SM operation in accordance with the change in operating wavelength.

To make a detailed study of cladding parameters, we have studied the effect of d_3, d_4, h_3 and h_4 on the leakage losses of first two modes. Fig. 4.3 shows the effect of leakage losses of E_{11}^x and E_{21}^x modes with d_3. The leakage loss of E_{21}^x mode is always larger than that of the E_{11}^x mode throughout the spectral range. With d_3 = 3 µm the waveguide introduces 0.945 dB/mm and 11.926 dB/mm losses to E_{11}^x and E_{21}^x modes respectively. Thus a 1.67 mm length of waveguide can strip off all higher-modes to ensure effective SM operation. A small value of d_3 (< 2 µm) introduces high leakage loss to E_{21}^x, however it also increases the fundamental loss beyond 1 dB/mm. Hence we fixed d_3 = 3 µm.

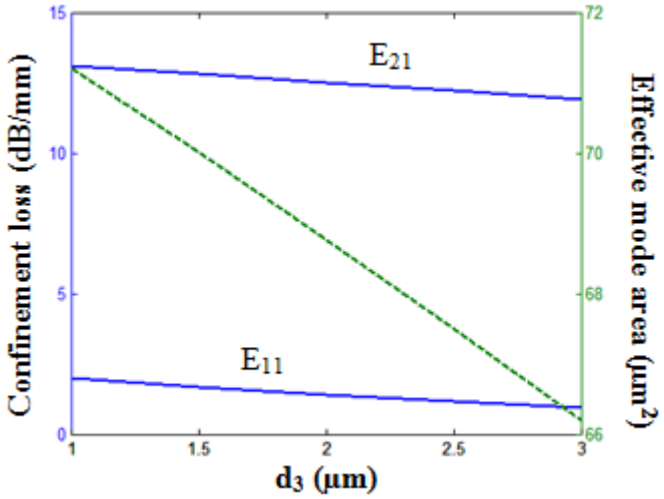

Fig. 4.3: Effect of cladding parameter d_3 on leakage loss and effective mode area of first two modes of the waveguide at 1.55 µm wavelength when a = 2 µm, h_3 = 5 µm, d_4 = 0.5 µm, h_4 = 7 µm.

Fig. 4.4 depicts the variation of leakage losses of E_{11}^{x} and E_{21}^{x}modes with d_4, and it is clear that at d_4 = 0.5 µm, the leakage loss of the first higher mode is quite high as compare to that of for fundamental mode.

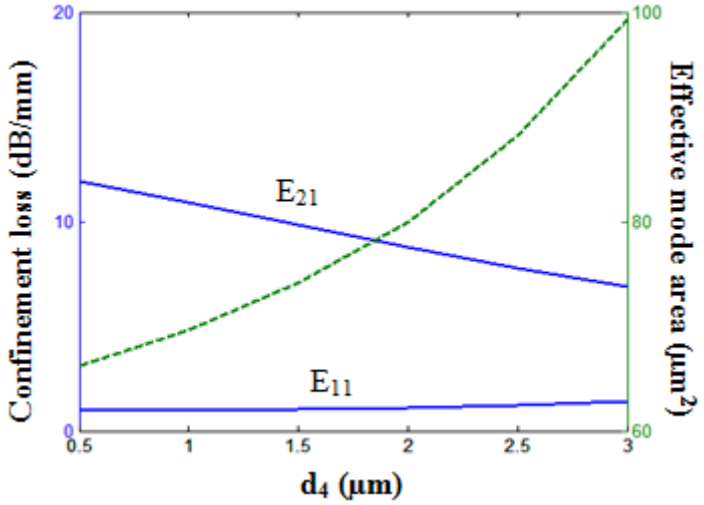

Fig. 4.4: Effect of cladding parameter d_4 on leakage loss and effective mode area of first two modes of the waveguide at 1.55 µm wavelength when a= 2 µm, d_3 = 1 µm, h_3 = 5 µm, h_4 = 7 µm.

Using a = 2 µm, d_3 = 3 µm, d_4 = 0.5 µm, the cladding parameter h_3 is varied and the effect of losses of the fundamental and first higher order modes have been observed. This feature of proposed structure has been shown in Fig.4.5. A peak in the leakage loss of the E_{21}^{x} mode is the signature of resonance coupling of this mode to high-index leaky cladding for a particular value of h_3. At h_3 = 4 µm, the fundamental mode offers leakage loss as low as 0.478 dB/mm while, the first higher order mode suffers with leakage loss as large as 19.689 dB/mm. Further increase in h_3 decreases the loss of the higher mode.

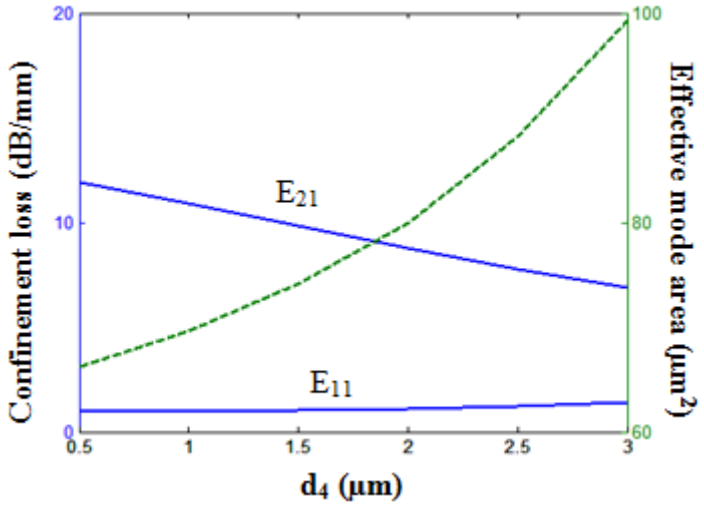

Fig. 4.5: Effect of cladding parameter h_3 on leakage loss and effective mode area of first two modes of the waveguide at 1.55 μm wavelength when a= 2 μm, d_4= 0.5 μm, d_3 = 1 μm, h_4 = 7 μm.

With a = 2 μm, d_3 = 3 μm, d_4 = 0.5 μm, h_3 = 4 μm, the cladding parameter h_4 is varied, and its effect on the leakage losses on the first two modes of the structure is shown in Fig. 4.6. At h_4 = 7 μm, the loss of fundamental loss is very less (< 1dB/mm) while, the waveguide introduces approximately 20 dB/mm loss to E_{21}^{x} mode which is able to show SM operation after passing only 1mm propagation length in the waveguide. This clearly shows the flexibility in designing the structure for LMA SM operation. At h_4 = 7 μm, the fundamental mode is confined in the core with a mode area of 50 μm^2.

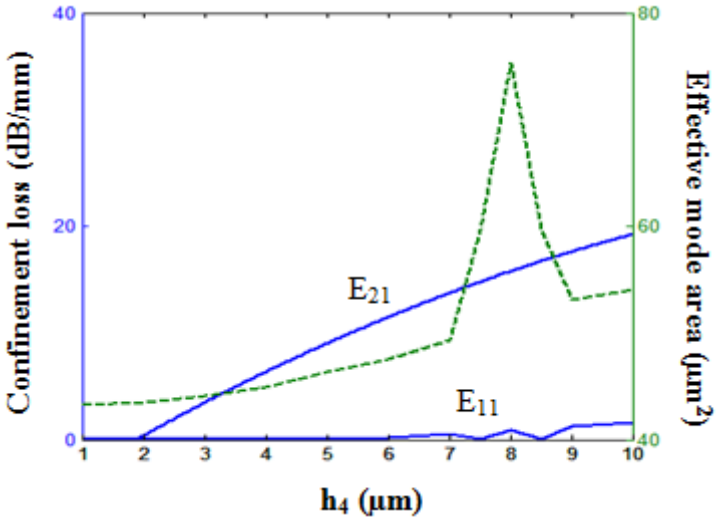

Fig. 4.6: Effect of cladding parameter h_4 on leakage loss and effective mode area of first two modes of the waveguide at 1.55 μm wavelength, when a= 2 μm, d_4= 0.5 μm, d_3 = 1 μm, h_3 = 4 μm.

4.4.1 Extended Single Mode Operation:

The proposed channel waveguide manifest SM operation due to dispersive cladding. The single mode operation characteristics of the waveguide have been explained by optimising the spectral variation of the leakage loss as shown in Fig. 4.7. The leakage loss of E_{21}^{x} mode is always greater than that of E_{11}^{x} mode throughout the spectral variation. At λ = 2.0 µm, E_{11}^{x} mode experiences 0.179 dB/mm, however, a 7 dB/mm loss is experienced by E_{21}^{x} mode at λ = 1.25 µm. Thus, a 2.6 mm long waveguide is able to signify the effective SM over the entire spectral range of 1.25 – 2.0 µm without instigating more than 1 dB loss to the fundamental mode. The core area of this channel waveguide structure is 50 µm^2. At λ = 1.55 µm, the E_{11}^{x} mode of waveguide suffers with 0.51 dB/mm leakage loss and E_{21}^{x} mode suffers with 11.75 dB/mm leakage loss. Therefore, 1.7 mm long waveguide can strip off all the higher-order modes and ensure effective SM operation at 1.55 µm.

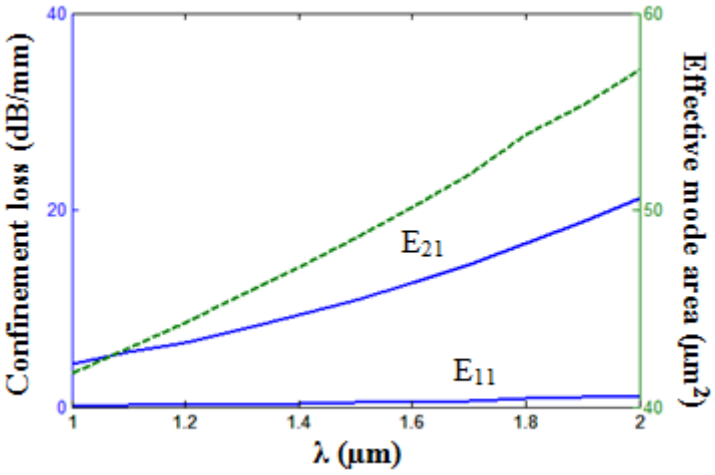

Fig. 4.7: The spectral variation of leakage losses on the leakage losses on the first two modes of the waveguide when a= 2 µm, d_4= 0.5 µm, d_3 = 1 µm, h_3 = 4 µm, h_4 = 7 µm.

CHAPTER 5

DESIGN AND ANALYSIS OF HIGHLY NONLINEAR CHALCOGENIDE RIB WAVEGUIDE FOR SLOW-LIGHT GENERATION

5.1 Introduction:

The velocity of light in vacuum, c is approximately 3×10^8 ms^{-1}, fast enough to make 7.5 round-the-world trips in a single second and to move a distance of 300 mm in 1 ns. This ultrahigh speed is advantageous for efficient data transmission between two points, whether they are separated on a global scale or on a single chip; however, it also makes control of optical signals in the time domain difficult. Slow-light is a technology now being investigated as a means to overcome this problem [37].

Slow-light refers to the condition $v_g << c$. In fact, group velocities smaller than 17 m/s and 57 m/s have been experimentally observed [38]. Slow-light is the research field that is gaining interest in the past few years because of several utilization in optical buffering, data synchronization, optical memories, optical signal processing, microwave photonics and precise interferometric instruments [38-40]. It is an important area of research that is of fundamental curiosity and has great potential for applications. The use of optical waveguides is particularly attractive for application since it can be readily integrated with existing technologies. There are many mechanisms through which slow-light can be generated, all of which create with high dispersion along with narrow spectral regions, i.e. peaks in the dispersion relation. Schemes are basically divided into three categories: Material dispersion, Inter-modal dispersion, Intra-modal dispersion. The slow-light has been recently manifested in optical waveguide and fibers by stimulated Brillouin scattering (SBS) [41-43] and stimulated Raman scattering (SRS) [44-45]. The slow-light technique based on SBS particularly of interest as it allows a very simple long-lasting implementation of tunable optical pulse delays, using mostly standard telecom components. There are three main features that make slow-light devices cynosure for engineering and other applications. The first is that, differently from material slow-light, the propogation occurs virtually without loss (or gain). In fact, in the material transparency window, the slow-light regime is separated

from the loss regime (i.e. the band–gap) [13, 46, 47, and 14]. The second advantage is that such devices can be realized with integrated photonic circuit technology, thus having the potential for large footprints and parallelization. Finally, only in structural slow-light energy velocity and so the enhancement of the nonlinear effects can be expected [48].

Heidari *et al.* showed and gave fundamentals of dispersion engineering of slow-light photonic crystal waveguide based on the selective microfluidic infiltration techniques [45]. At the recent time, Pant *et al.* reported first time the maximum delay of ~23 ns in 7 cm long chalcogenide rib waveguide [46]. Schneider *et. al.* proposed a step index optical fibre in silica material for generation of millimetre waves [13]. For this purpose, a lot of work has been performed to lessen the length of the fibre by selecting a higher refractive index media [48-50]. *Monat et al.* presented a similar study on various nonlinear phenomenon enhanced by slow-light in silicon based photonic crystal waveguide [45]. The SBS modelling in standard silica fibres for slow-light applications has been made earlier in different research and review articles [51-55]. Recently, photonic crystal fibre pumped with 140 mW was achieved by using 1 m long tellurite material [56].

As we know that the chalcogenide glasses have high third-order nonlinearity, therefore it can be used as a functional optical fibre, along with all non-silica glasses, are also the excellent applicant for infrared transmission. The intrinsic, material loss of As_2Se_3 chalcogenide glass is very less in infrared region which makes it attractive for the use in the infrared transmission, optical fibres for optical sensors and telecommunications [57]. In spite of very low loss in infrared region, As_2Se_3 chalcogenide glass possesses very high linear and nonlinear refractive index which increases it capability as a promising candidate for nonlinear applications such as slow-light and supercontinuum generation [58].

Design and analysis of As_2Se_3 based chalcogenide waveguide for tunable slow-light generation based on stimulated Brillouin scattering. The intrinsic material properties of As_2Se_3 based on chalcogenide material have been taken from Ref. [58-59]. The influences of waveguide characteristics such as maximum pump power for undistorted output pulse and time delay experienced by the pulse have been simulated numerically. Our simulated results indicate that the time delay accomplished by the pulse in proposed structure can be adjusted with the pump power [60] and thereby tunable slow-light features can be obtained from proposed waveguide structure.

5.2 Design of proposed rib waveguide:

To study the slow-light generation in Rib waveguide based on stimulated Brillouin scattering firstly, we have proposed a single mode Rib waveguide structure. The transverse cross-sectional view of proposed design has been shown in Fig. 5.2. It consists of As_2Se_3 based chalcogenide glass core of refractive index n_1, width $2a$ and height h is formed on a substrate with lower refractive index n_2 which consists of As_2S_3 of refractive index equal to 2.45. The cladding is made by air of refractive index n_3. The refractive index of As_2Se_3 based chalcogenide glass has been taken equal to 2.815 at 1.55 μm. Thus, in my design I have arranged the width and height of the core and calculated its nonlinear properties. From the modeling point of view the designed structure can be fabricated by standard ion etching methods.

Table. 5.1: Optical properties of As_2Se_3 based chalcogenide glass at 1.55 μm

Parameters	**Chalcogenide (As_2Se_3)**
Refractive index, n	2.815
Brillouin gain coefficient, g_B (m/W)	6.75×10^{-9}
Brillouin gain bandwidth, Δv_B(MHz)	13.2
Loss (dB/m)	0.90

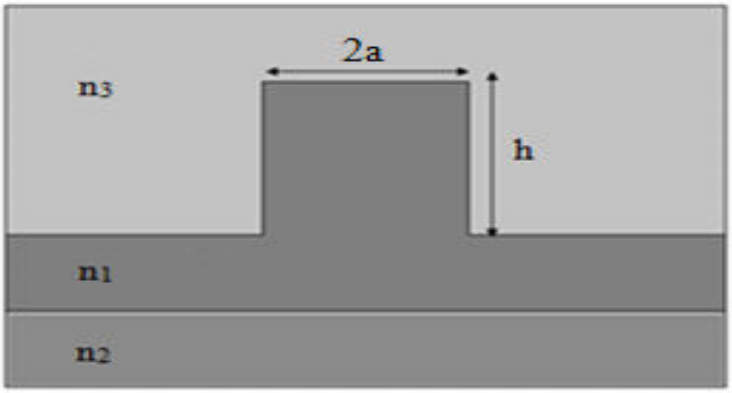

Fig. 5.1: Transverse cross-sectional view of proposed highly nonlinear waveguide.

5.3 Numerical Results and Discussion:

For the simulations, in order to ensure single mode operation in proposed rib waveguide, the value of half-width of waveguide (i.e. *a*) is chosen equal to 2 µm and that of height of the core (i.e. *h*) is as 4 µm in following simulations. The value of polarization factor is taken to be 0.667. The simulations have been carried out at 1.55 µm operating wavelength. The minimum input pump power for initiation of SBS effect and maximum pump power for undistorted output is found to be 0.058 mW and 588 mW respectively.

The effective mode area plays very important role in enhancing nonlinear effects in optical waveguide. In this work the effective mode area of rib waveguide has been controlled by tuning the half-width of waveguide. The impact of the half-width on the effective mode area of propagating mode has been illustrated in Fig. 5.2. The effective mode area increases with increasing the half width of the waveguide.

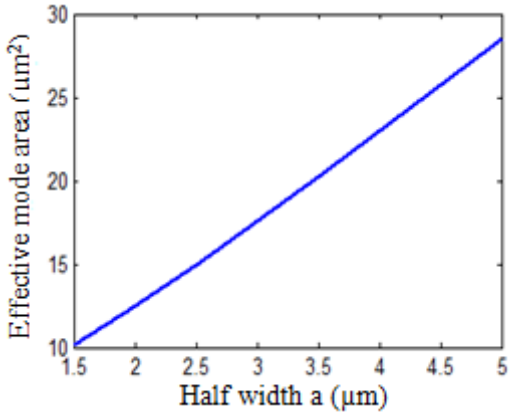

Fig. 5.2: Variation of Effective mode area with half width of waveguide.

The confinement loss is also a very important feature of optical waveguide. As illustrated in Fig. 5.3, the maximum confinement loss is 0.4287 dB/m at a =1.5 µm and it decreases on increasing the value of a.

For optimum single mode operation with low confinement loss, we have taken the core half width as 2 µm and core height as 4 µm. For these value, we have found that the effective mode area of the waveguide to be 12.51 μm^2. The electric field distribution of the fundamental mode of the proposed structure is shown in figure 5.4 at 1.55 µm. It can be observed that the propagating mode is well confined within the core of the rib waveguide.

As illustrated in Fig. 5.5, the effective mode area of propagating mode increases linearly on increasing the value of the core-height of the rib waveguide structure. The simulated results show that the effective mode area can be obtained as 9.40 μm^2 and 16.19 μm^2 at core height of 2 µm and 6 µm respectively.

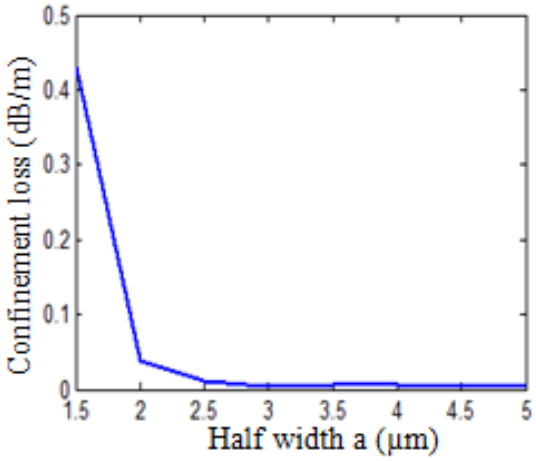

Fig. 5.3: Variation of Confinement loss with half width of waveguide.

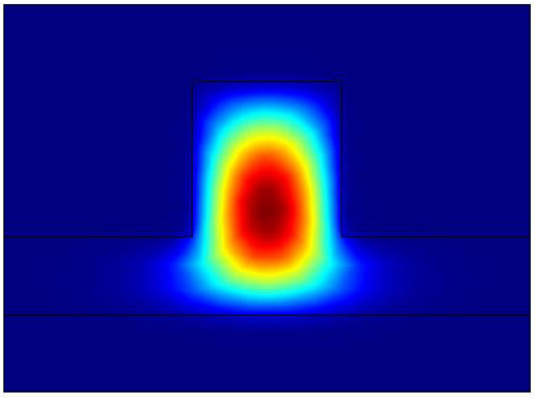

Fig. 5.4: Electric field distribution of fundamental mode with a = 2 µm and h = 4 µm at 1.55 µm wavelength.

The electric field distribution is the functional and analytical representation which denotes the single mode operation of the proposed rib waveguide structure at a wavelength of 1.55 µm with half width and core height of the waveguide as 2 µm and 4 µm respectively. The large refractive index of the chalcogenide glass resulting in the strong optical and acoustic confinement in the rib structure, providing large light-sound interaction and reduced optical mode area A_{eff}, which further improves the intensity of pump at relatively low power.

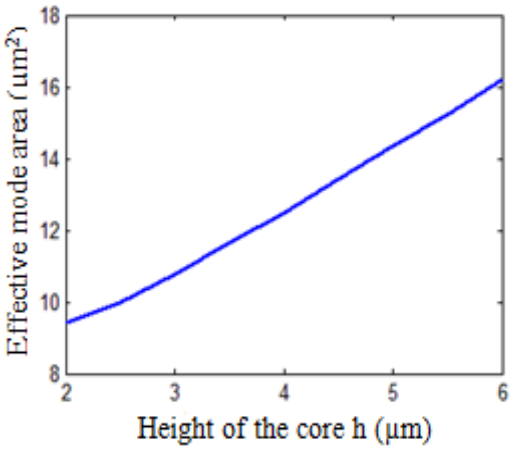

Fig. 5.5: Variation of Effective mode area with core height of the waveguide.

Confinement loss as a function of core height of the rib waveguide is shown in Fig. 5.6. By varying the core height it can be analysed that the confinement loss decreases exponentially on increasing the value of core-height. The minimum confinement loss is equals to 3.7×10^{-3} dB/m at h = 6 μm and a = 4 μm.

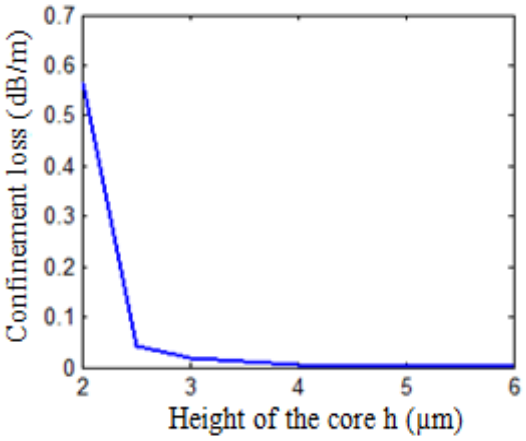

Fig. 5.6: Variation of Confinement loss with core height of the waveguide.

The effect of the variation of the Brillouin gain on the time-delay of the pulses is shown in Fig. 5.7. The time-delay increases on increasing Brillouin gain.

The influences of pump power on time-delay per unit length at a = 2 μm and h = 4 μm have been illustrated in Fig. 5.8. The time-delay which is desired can be achieved by tuning the pump power for a given structure. For example time-delay can be tuned upto ~252 ns by varying the pump power upto 588 mW in 10 cm long rib waveguide. At this pump power, for a waveguide of 10 cm length, time-delay is calculated to be ~252 ns. Time-delay in output

pulse increases linearly with increasing pump power. The FOM of the proposed waveguide design is estimated as 553.75 at pump power of 588 mW.

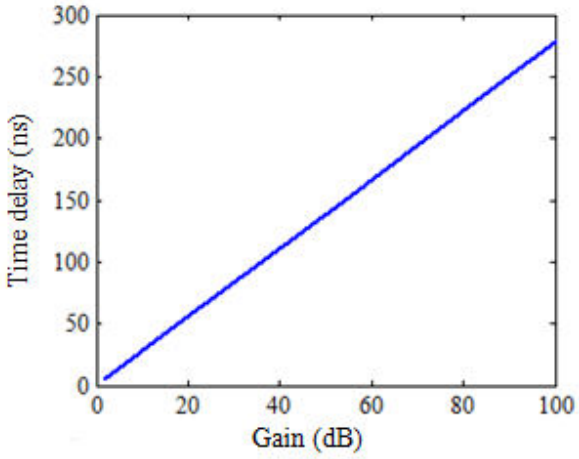

Fig. 5.7: Variation of time-delay with respect to gain.

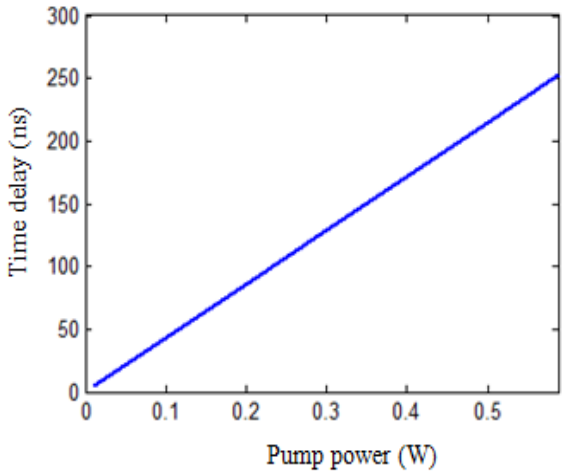

Fig. 5.8: Variation in the time-delay per unit length with incident pump power.

CHAPTER 6

CONCLUSION AND SCOPE FOR FUTURE WORK

6.1 Conclusion:

The proposed design which is a large core area rectangular channel waveguide structure, offers effective single mode operation. The waveguide consists of a uniform rectangular large-core and the low-index trench assisted leaky multi-cladding to provide leakage for all the modes. When all the modes, except for the fundamental mode, are stripped off sufficiently in the waveguide, effective single mode is ensured. We have carried out a design study of the waveguide for obtaining high differential leakage loss between the first two modes to ensure effective SM operation. Our numerical results show SM operation of the structure with a mode area larger than **50 µm^2** can provide effective SM operation over the spectral range from **1.25 – 2.0 µm**. A Waveguide that introduces a sufficiently high leakage loss to the higher order mode, (E_{21}^{x} > 5 dB/mm) and a nominal loss to the fundamental mode (E_{11}^{x}<1dB/mm) would be appropriate for effective SM operation which is capable of suppressing the nonlinear effects and is expected to find applications in the design of high-powered waveguide laser and amplifiers.

The second proposed design is a highly nonlinear As_2Se_3 chalcogenide optical waveguide for tunable slow-light based on stimulated Brillouin scattering. Such a waveguide utilises a cladding which can be easily fabricated by reactive ion etching technique. The effective mode area and confinement loss has been calculated for different values of half width and core height of the optical waveguide. The waveguide characteristics for slow-light such as maximum allowable pump power, Brillouin gain and time delay experienced by the pulse for proposed waveguide has been calculated. Brillouin gain as much as ~209 dB/m and maximum time delay as much as **~252 ns** has been achieved for a 10 cm long designed rib waveguide pumped with 588 mW.

6.2 Scope for Future Work:

The proposed LMA waveguide can be used as a laser and amplifier cavity after doping with rare earth metal like Erbium and Yttrium and its performance can be determine in application

such as optical fibre communications, high power optical amplifiers, high power fibre lasers, nonlinear devices, power transmission and other exciting areas. The slow-light can be enhanced by taking pump with larger power. It will provide promising solutions for tunable and broadband time delay or phase shift lines, for microwave and millimetre wave systems. This demonstration opens up on-chip SBS devices and the depicted chalcogenide waveguide is anticipated to have probable applications in attainment of dense slow-light devices.

Moreover, the enhancement of nonlinearity and the capability of storing light provide promising routes towards achieving on-chip all-optical signal processing in photonics devices. The long term reliability and impact resistance of all-fibre components can be improved by suitably adapting the primary and secondary packaging schemes. Devices fabricated with new design exhibits better performance in temperature cycling, humidity aging and drop tests. Biomedical systems also need many novel all-fibre components.

REFERENCES

1. M. J. Adams, An Introduction to Optical waveguides. New York: Wiley, 1981.
2. R.A. Soref, J. Schmidtchen, and K. Petermann, "Large single mode RIB waveguides in GeSi-Si and Si-on-SiO_2," IEEE J. Quantum Electron., vol. 27, pp. 1971-1974, 1991.
3. K. Petermann, "Properties of optical RIB waveguides with large cross section," Archiv fur Electronik and Ubertragungstechnik, vol. AEU-30, pp. 139-140, 1976.
4. S.P. Pogossian, H. L. Gall, J. Gieraltowski, and J. Loaec, "Determination of the parameters of rectangular waveguides by new effective index methods ," J. Modern opt. Vol. 42, no. 5, pp. 403-409, 1995.
5. Zon, X. Y., M. I. Hayee, S. M. Hwang, and A. E. Wilner, "Limitations in 10 – Gb/s WDM optical fibre transmission when using a variety of fibre types to manage dispersion and nonlinearities," J. Lightwave Tech, vol. 14, 1144-1152, 1996.
6. J. Capmany, I. Gasulla, and S. Sales, "Microwave Photonics: Harnessing the speed of light", Nature photonics, vol 5, p731, 2011.
7. M. Santagiustina, "Electromagnetic Energy Velocity in Slow-light", *Proc. Slow and fast light Tropical Meeting*, paper SLTuB5, 2011.
8. K. S. Abedin, "Observation of strong stimulated Brillouin scattering in single mode As_2Se_3 chalcogenide fibre, *Opt. Exp. 13*, 10266-10271.
9. L. Thevenaz, "Slow and fast light in optical fibres", *Nature photon*. 2, 474-481.
10. G. M. Gehring, R. W. Boyd, A. L. Gaeta, D. J. Gauthier, A. E. Wilner, "Fibre-based slow-light technologies", J. Lightwave Technol. 26(23), 3752-3762, 2008.
11. K. S. Abedin, "Stimulated Brillouin scattering in single mode tellurite glass fibre", Opt. Exp., 14(24), 11766-11772, 2006.
12. T. S. Saini, A. Kumar, R. K. Sinha, "Slow-light generation in a single mode tellurite fibres", J. Modern Optics. 62(7), 508-513, 2015.
13. T. Schneider, D. Hannover, and M. Junker, "Investigation of Brillouin scattering in optical fibres for the generation of millimetre waves", *J. Lightw. Tech*. 24, 295-304.

14. P. E. Pace, C. C. Foster, "Beam propagation analysis of a parallel configuration of Mach-Zender interferometers", Optical Engineering, vol 33, pp.2911-2921, 1994.

15. M. N. O. Sadiku, "A simple introduction to finite element analysis of electromagnetic problems", IEEE Trans. Educ., vol. 32, no.2, May, pp. 85-89, 1989.

16. K. S. Yee, "Numerical solution of initial boundary-value problems involving Maxwell's equations in isotropic media", IEEE Trans. Ant. Prop., vol. AP-14, May, pp.302-307, 1966.

17. J. I. Mackenzie, IEEE J. Sel. Top. Quantum Electron. 13, 626, 2007.

18. J. M. Eggleston, T. J. Kane, K. Kuhn, J. Unternahrer, R. L. Byer, IEEE J. Quantum Electron, 20, 289, 1984.

19. C. L. Bonner, C. T. A. Brown, D. P. Shepherd, W. A. Clarkson, A. C. Tropper, D. C. Hanna, B. Ferrand, Opt. Lett. 23, 942, 1998.

20. C. Zumdzinki, D. Botez, L. J. Mawat, A. Bhattacharya, M. Nesnidal, R. F. Nabiev, IEEE J. Sel. Top. Quantum Electron. 1, 129, 1995.

21. D. P. Shepherd, S. J. Hettrick, C. Li, J. I. Mackenzie, R. J. Beach, S.C. Mitchell, H. E. Meissner, J. Phys. D Appl. Phys. 34, 2420, 2001.

22. J. N. Walpole, J. P. Donelly, P. J. Taylor, L. J. Missaggia, C. T. Harris, R. J. Bailey, A. Napoleone, S. H. Groves, S. R. Chin, R. Huang, J. Plant, IEEE Photon, Technol. Lett. 14, 756, 2002.

23. R. K. Huang, L. J. Missaggia, J. P. Donnelly, C. T. Harris, G. W. Turner, IEEE Photon. Technol. Lett. 17, 959, 2005.

24. S. Yin, K. W, Chung, H. Liu, P. Kurtz, K. Reichard, Opt. Commun. 177. 225, 2000.

25. N. G. R. Broderick, H. L. Offerhaus, D. J. Richardson, R. A. Sammut, J. Caplen, L. Dong, Opt. Fibre Technol. 5. 185, 1999.

26. Y. Jeong, J. K. Sahu, D. N. Payne, J. Nilsson, Opt. Express 12, 6088 (2004).

27. H. L. Offerhaus, N. G. Broderick, D. J. Richardson, R. Sammut, J. Caplen, L. Dong, Opt. Lett 2, 1683, 1998.

28. G. P. Lees, D. Taverner, D. J. Richardson, L. Dong, T. P. Newson, Electron. Lett 33, 393, 1997.

29. N. G. R. Broderick, D. J. Richardson, D. Taverner, J. E. Caplen, L. Dong, M. Lbsen, Opt. Lett 24, 566, 1999.

30. A. Kumar, V. Rastogi and K. S. Chaing, "Leaky optical waveguide for high power applications", Appl. Phys. B 85, 11-16, 2006.

31. A. Kumar, V. Rastogi, and K. S. Chaing, "Large core single mode channel waveguide based on geometrically shaped cladding", Appl. Phys. B. 90, 507-512, 2008.

32. A. Kumar, V. Rastogi, "Multilayer cladding leaky planer waveguide for high power applications", Appl. Phys B 92, 577-583, 2008.

33. A. Kumar, V. Rastogi, "Design and analysis of dual-shape core large mode area optical fibre", App. Opt. 50, E119-E124, 2011.

34. P. Wang, L. J. Copper, R. B. William, J. K. Sahu, and W. A. Clarkson, "Helical core ytterbium doped fibre laser", Electron. Lett. 40, 1325-1326, 2004.

35. P. Wang, L. J. Copper, J. K. Sahu, and W. A. Clarkson, "Efficient single mode operation of cladding pumped ytterbium doped helical fibre laser", Opt. Lett. 31, 226-228, 2006.

36. J. P. Koplow, D. A. V. Kliner, and L. Golberg, "Single mode operation of a coiled multimode fibre amplifier", Opt. Lett. 25, 442-444, 2000.

37. T. Baba, Nature Photon, 2, 465-473, 2008.

38. L. V. Hau, S. E. Harris, Z. Dutton, C. H. Behroozi, "Light speed reduction to 17 meters per second in an ultracold atomic gas", Nature, vol. 6027, p594, 1999.

39. S. Rawal, R. K. Sinha, and R. M. De La Rue, " Slow-light miniature devices with ultra-flattened dispersion in silicon-on-insulator photonic crystal, *Opt. Exp. 17*, 13315-13325.

40. J. Sharping, Y. Okawachi, and A. Gaeta, "Wide bandwidth slow-light using a Raman Fibre amplifier, *Opt. Exp. 13*, 6092-9098.

41. L. Y. Ren and Y. Tomita, "Transient and nonlinear analysis of slow-light pulse propagation in an optical fibre via stimulated Brillouin scattering, *J. Opt. Soc. Am. B* 26, 1281-1288.

42. S. H. Wang, L. Y. Ren, Y. Liu, and Y. Tomita, "Zero-broadening SBS slow-light propagation in an optical fibre using two broadband pump beams, *Opt. Exp. 16*, 8067-8076.

43. D. Dahan, and G. Eisenstein, "Tunable all optical delay via slow and fast light propagation in a Raman assisted fibre optical parametric amplifier: a route to all optical buffering, Opt. Exp. 13, 6234-6248.

44. E. P. Ippen, and R. H. Stolen, "Stimulated Brillouin scattering in optical fibres", *Appl. Phys. Lett. 21*, 539-540.

45. M. E. Heidari, C. Grillet, C. Monet, and B. J. Eggleton, "Dispersion engineering of slow-light photonic crystal waveguide using microfluidic infiltrations, Opt. Exp. 17(3), 1628-1635, 2009.

46. R. Pant, A. Byrnes, C. G. Poulton, E. Li, D. Y. Choi, S. Madden, B. L. Davis, and B. J. Eggleton, "Photonic-chip-based tunable slow and fast light via stimulated Brillouin scattering, Opt. Lett. 37 (5), 969-971, 2012.

47. C. Monat, B. Coreoran, D. Pudo, M. E. Heidari, C. Grillet, M. D. Pelusi, D. J. Moss, B. J. Eggleton, T. P. White, L. O. Faolain, and T. F. Krauss, "Slow-light Enhanced Nonlinear optics in silicon Photonic Crystal Waveguides, *IEEE J. Sel. Top. Quant. Elect*. 16, 344-356, 2010.

48. G. Qin, H. Sotobayashi, M. Tsuchiya, A. Mori, T. Suzuki and Y. Ohishi, Stimulated Brillouin scattering in a single mode tellurite fibre for amplification, lasing and slow-light generation, *J. Lightw. Tech. 26*,492-498, 2008.

49. K. S. Abedin, G. W. Lu and T. Miyazaki, Slow-light generation in single mode Er-doped tellurite fibre, *Electron. Lett. 44(1),* 16-U21, 2008.

50. M. O. Van, Deventer and A. J. Boot, Polarization properties of stimulated Brillouin scattering in single mode fibres, *J. Lightw. Tech. 12(4)*, 585-590, 1994.

51. J. B. Khurgin and R. S. Tucker, Eds ., *Slow-light: Science and Applications*, CRC Press, Boca Raton, 2008.

52. J. T. Mock and B. J. Eggleton, Expect more delays, Nature, 433, 811-812, 2005.

53. Z. Zhu, D. J. Gauthier, Y. Okawachi, J. E. Sharping, A. J. Gaeta, R. W. Boyd, and A. E. Wilner, Numerical study of all-optical slow-light delays via stimulated Brillouin scattering in an optical fibre, *J. Opt. Soc. Am.* B 22(11), 2378-2384, 2005.

54. V. P. Kalosha, L. Chen, and X. Bao, Slow and fast light via SBS in optical fibres for short pulses and broadband pump, *Opt. Exp. 14(26),* 12693-12703, 2006.

55. S. Hou, Z. Wang , Y. Shang Y. Liu, J. Lei, and Y. Xu, Influence of SBS gain coefficient on time delay and pulse broadening in fibres, PIERS Proceedings, Suzhou, China, September 12-16, 938-942, 2011.

56. T. S. Saini, A. Kumar, R. K. Sinha , Stimulated Brillouin scattering based tunable slow-light in tellurite photonic crystal fibre, Proc. Photonics 2014: 12th international Conference on Fibre optics and Photonics @ OSA, IIT Kharagpur, WB, India, December 13-16,2014, T3A.28, 2014.

57. V. Shiryaev, and M. Churbanov, Trends and Prospects for development of chalcogenide fibres for mid-infrared transmission, *J. Non-cryst. Solids 377, 225-230,* 2013.

58. B. J. Eggleton, B. L, Davies, and K. Richardson, Chalcogenide photonics, *Nature Photon. 5,* 141-148, 2011.

59. K. Ogusu, H. Li, and M. Kitao, "Brillouin-gain coefficients of chalcogenide glasses", *J. Opt. Soc. Am. B 21,* 1302-1304, 2004.

60. T. Baba, Light propagation characteristics of straight single line defect optical waveguides in a photonic crystal slab fabricated into a silicon-on-insulator substrate. *IEEE J. Quant. Electron.* 38, 743-752, 2002.